

Published in final edited form as:

*Adv Healthc Mater.* 2013 September ; 2(9): 1224–1228. doi:10.1002/adhm.201200380.

## μHall Chip for Sensitive Detection of Bacteria

David Issadore<sup>1,†</sup>, Hyun Jung Chung<sup>1,†</sup>, Jaehoon Chung<sup>1</sup>, Ghyslain Budin<sup>1</sup>, Ralph Weissleder<sup>1,2,\*</sup>, and Hakho Lee<sup>1,\*</sup>

<sup>1</sup>Center for Systems Biology, Massachusetts General Hospital, 185 Cambridge St, CPZN 5206, Boston, MA 02114

<sup>2</sup>Department of Systems Biology, Harvard Medical School, Boston, MA 02115

### Abstract

Sensitive, rapid and phenotype-specific enumeration of pathogens is essential for the diagnosis of infectious disease, monitoring of food chains, and for defense against bioterrorism.

Microbiological culture and genotyping, techniques that sensitively and selectively detect bacteria in laboratory settings, have limited application in clinical environments due to high cost, slow response times, and the need for specially trained staff and laboratory infrastructure. To address these challenges, we developed a microfluidic chip-based micro-Hall (μHall) platform capable of measuring single, magnetically tagged bacteria directly in clinical specimens with minimal sample processing. We demonstrated the clinical utility of the μHall chip by enumerating Gram-positive bacteria using a two-step bioorthogonal labeling procedure. The overall detection limit of the system was similar to that of culture tests (~10 bacteria), but the assay time was 50-times faster. This low-cost, single-cell analytical technique is especially well-suited to diagnose infectious diseases in resource-limited clinical settings.

### Keywords

μHall; bacterial detection; magnetic nanoparticles

---

Development of fast, sensitive, and accurate diagnostic tests is key to controlling infectious diseases.<sup>[1–3]</sup> By enabling early diagnosis and treatment, such tests would not only help rapidly identify sources of infection, but would prevent further disease transmission, and reduce the risk of patients developing long-term complications.<sup>[2]</sup> The detection of pathogens (bacteria, parasites, fungi, viruses) in clinical specimens, however, has continued to present significant technical challenges, namely because a) specimens often have a complex composition (e.g., blood, tissue), b) sample sizes are often limited, and c) specimens may contain very few pathogens (e.g., early disease stages).<sup>[4–7]</sup> Magnetic sensing, a technique in which pathogens are labeled with magnetic nanoparticles (MNPs), is

---

Corresponding authors: H. Lee, PhD, Center for Systems Biology, Massachusetts General Hospital, 185 Cambridge St, CPZN 5206, Boston, MA, 02114, 617-726-8226, hlee@mgh.harvard.edu. R. Weissleder, MD, PhD, Center for Systems Biology, Massachusetts General Hospital, 185 Cambridge St, CPZN 5206, Boston, MA, 02114, 617-726-8226, rweissleder@mgh.harvard.edu.

<sup>†</sup>These authors contributed equally.

Supporting Information

Supporting Information is available from the Wiley Online Library or from the author.

uniquely well suited to addressing these challenges.<sup>[8–12]</sup> The inherently negligible magnetic background of biological samples enables highly sensitive measurements to be obtained without the need for sample purification. Bacterial loss prior to measurement is thus minimized and the assay procedure significantly simplified for clinical use.<sup>[13,14]</sup> Furthermore, magnetic sensors can be easily miniaturized and integrated onto low-cost chips for portable use in clinical settings.

We herein present a new magnetic sensor platform for bacterial detection, which combines the benefits of both magnetic measurements and single-cell detection accuracy. In this approach, target bacteria are first labeled with molecular-specific magnetic nanoparticles (MNPs), which are subsequently detected by miniaturized Hall ( $\mu$ Hall) sensors. In previous work, we used a prototype  $\mu$ Hall system to detect mammalian cells ( $> 10 \mu\text{m}$  in diameter) under flow conditions.<sup>[10]</sup> Adapting the  $\mu$ Hall technology to the detection of bacteria in the present study, however, was challenging due to the much smaller size of bacteria ( $\sim 1 \mu\text{m}$ ). We addressed this problem in two ways: 1) by implementing a new microfluidic system, which could reliably stream individual bacteria to the sensor surface; and 2) by employing bacterial labeling techniques based on bioorthogonal nanoagents to achieve efficient and maximal MNP-loading on bacterial targets.<sup>[13]</sup> We subsequently validated the developed platform by performing bacterial counts and by detecting Gram-positive bacteria in unprocessed samples.

The  $\mu$ Hall platform offers several key advantages that enable sensitive detection of pathogens in clinical samples. Because the chip can detect individual pathogens, it is able to ignore not only unbound MNPs but also other cells with inadvertently attached MNPs. Consequently, the chip is insensitive to non-specific labeling and requires no washing steps to remove excess reagents. Additionally, the entire measurement is performed on a single microfluidic chip format, which eliminates the need for laboratory infrastructure and trained personnel. The assay could be adapted to differentiate a variety of other bacterial species by changing the affinity ligands. With such capacities, the  $\mu$ Hall platform thus represents a comprehensive and universal diagnostic platform with potentially broad clinical applications in resource-limited, point-of-care settings.

Figure 1a illustrates the assay scheme. Bacteria in solution were initially labeled with MNPs targeting specific molecular surface markers; this rendered bacteria superparamagnetic. Consequently, when subjected to external magnetic fields, each bacterium assumed a magnetic moment  $m$ , which was proportional to the number of expressed biomarkers  $N$  and the magnetic moment of the MNPs  $m_p$ , ( $m = N \times m_p$ ). The local magnetic fields emanating from individual bacteria were then measured by the  $\mu$ Hall sensors, with peaks in Hall voltage ( $V_H$ ) occurring as single bacteria flowed over the sensor.

To obtain efficient MNP-loading on target bacteria, a two-step bioorthogonal labeling method was employed.<sup>{Haun et al., 2010, Nat Nanotechnol, 5, 660-5}</sup> In this strategy, bacterial targets were first labeled with affinity ligands modified with *trans*-cyclooctene (TCO), and MNPs modified with 1,2,4,5-tetrazine (Tz) were then applied. MNPs were thus coupled to the labeled bacterial targets via a cycloaddition reaction between Tz and TCO.<sup>[15,16]</sup> The method is fast, modular, and can be applied to a variety of different

bacterial species using a generic MNP for labeling. Additionally, this method has been shown to maximize MNP binding onto targets<sup>[17,18]</sup>; each affinity ligand has multiple TCO tags, thereby providing multiple binding sites for MNPs. Indeed, compared to using direct ligand-MNP conjugates, this two-step method results in much higher (>600%) MNP loading onto target cells. {Chung et al., 2011, ACS Nano, 5, 8834-41} Figure 1b shows an example of such bacterial labeling. Vancomycin, an antibiotic that binds to the D-Ala-D-Ala moieties in the peptidoglycan of the bacterial cell wall of Gram positive bacteria was used as a targeting ligand. *Staphylococcus aureus* (*S. aureus*), a Gram-positive strain, was then labeled by vancomycin-TCO (vanc-TCO; Fig. S1a), and subsequently incubated with MNP-Tz (see Experimental section for details). This labeling technique resulted in dense particle-loading onto the bacterial surface (Fig. 1c) with  $\sim 10^5$  MNPs per cell. MNP loading without vanc-TCO incubation, however, was negligible (Fig. S1b), thus demonstrating the high specificity of the the bioorthogonal labeling procedure.

We adapted the  $\mu$ Hall system for robust bacterial detection. The device has a hybrid microfluidic/semiconductor chip structure, consisting of a microfabricated sensor and a hydrodynamic flow-focusing fluidic channel (Fig. 2a). An external magnetic field ( $B_0 \sim 0.5$  T), provided by a small neodymium magnet ( $\sim 1$  cm<sup>3</sup>; attached below the chip), was used to fully magnetize the MNPs. The design of this sensor was based on our initial  $\mu$ Hall prototype (see SI Methods).<sup>[10]</sup> In the current device, eight Hall elements, each with an active area of  $8 \times 8$   $\mu\text{m}^2$ , were laid out in an overlapping  $2 \times 4$  array (Fig. 2b). This geometry enabled more accurate bacterial counting, since it ensured that each bacterium passed over at least two  $\mu$ Hall elements. It was then possible to enhance the detection accuracy further by averaging the Hall voltages from all eight sensors. The mean Hall voltage ( $\langle V_H \rangle$ ) was thus shown to be proportional to the total magnetic moment ( $m$ ) of a single passing magnetic object, and independent of its size.<sup>[10]</sup> Compared to mammalian cancer cells, however, bacteria are assumed to have an approximately 100-fold lower  $m$ , due to their smaller surface area (diameter  $\sim 1$   $\mu\text{m}$ ) than mammalian cells (diameter  $\sim 10$   $\mu\text{m}$ ). To compensate for this loss in  $m$ , we devised a way to bring bacteria nearer to the Hall sensors. Given that  $V_H$  is proportional to  $\sim d^{-3}$ , where  $d$  is the distance between the center of a bacterium and the Hall sensor, bringing the bacteria closer to the sensors considerably boosts the signal-to-noise ratio (SNR; Fig. 2c). Indeed, our numerical simulation (see SI Methods) showed that the  $V_H$  was >1000-fold larger for a bacterium placed on the sensor surface ( $d = 0.5$   $\mu\text{m}$ ) than for a bacterium placed at the center of the microfluidic channel ( $d = 7.5$   $\mu\text{m}$ ).

To stream individual bacteria near to the Hall sensors, we used a two-stage flow focusing structure.<sup>[19]</sup> Cells were confined in the vertical direction, towards the bottom of the fluid channel, via a vertical sheath flow, and directed laterally towards the center of the fluid channel via coplanar sheath flows. This channel design was iteratively optimized through finite element simulations (Fig. 2d) until the sample flow could be confined within 2  $\mu\text{m}$  above the sensor surface. The final structure measured 200  $\mu\text{m}$  wide and 15  $\mu\text{m}$  high, and could operate under a flow rate of up to 2 ml/hour. Moreover, the use of hydrodynamic focusing allowed the physical channel to be much larger than bacteria, which in turn helped lower the fluidic resistance and reduce the risk of channel clogging. Cell-confinement could

be controlled by adjusting the relative flow rates of the lateral and vertical sheaths (Fig. 2e). We tested this design by detecting MNP-labeled *S. aureus* in-flow. With the use of flow-focusing, we were able to observe a distinct  $V_H$  peak (SNR  $\sim 50$ ) from a single bacterium (Fig. 2f). The flight time of the bacterium over the sensor was 20  $\mu$  seconds, and the estimated flow speed was  $\sim 1$  m/second. Without the use of flow focusing, however, the Hall voltage level fell below the noise floor of the device (2  $\mu$ V).

We next evaluated the analytical capacity of the  $\mu$ Hall system by comparing  $\mu$ Hall measurements with those from flow cytometry, for which bacterial samples were prepared by labeling *S. aureus* with fluorescent MNPs. The measured  $V_H$  distribution (from  $N = 5,000$  bacteria) obtained by the  $\mu$ Hall system was found to correspond well with measurements by flow cytometry (Fig. 3a) and thus confirmed the accurate detection of bacterial magnetic moments by the  $\mu$ Hall system. Importantly, because the  $V_H$  histogram obtained by the  $\mu$ Hall system was positioned well above the noise floor of the device, it ensured that all bacteria in the sample would be counted. Indeed, when we used samples with known bacterial concentrations, we obtained excellent agreement with expected bacterial counts ( $R^2 > 97\%$ ; Fig. 3b) over a wide dynamic range ( $10^1 - 10^6$  counts). It is possible that the deviation observed at low bacterial counts are due to errors arising from the preparation of spiked-samples. Since the  $\mu$ Hall system is capable of measuring individual bacteria, the detection limit is ultimately one bacterium.

The  $\mu$ Hall measurements are robust against biological backgrounds, as the sensing mechanism is based on magnetic interactions. Furthermore, measurements could be performed even in the presence of unbound MNPs. The  $\mu$ Hall sensors detect magnetic moments arising from a very small volume ( $\sim 10$  pL) which contains on average less than 1 unbound MNP (for a particle concentration of  $10^8$ /mL). Pathogens, in contrast, can have  $10^4 - 10^6$  MNPs per cell, generating dominant  $\mu$ Hall signal. To test this hypothesis, we compared  $\mu$ Hall detection of bacteria in both pure buffer (phosphate buffer saline; PBS) and in the presence of excess MNPs ( $10^9$  particles/ml). We confirmed that Hall voltages from both samples were similar (Fig. 3c). The slight increase in  $V_H$  ( $\sim 7\%$ ) observed in the presence of excess MNPs is presumed to be the result of longer exposure of bacteria to the MNPs, an effect that could be compensated for in post-data processing. In view of such background insensitivity, direct pathogen detection is possible. This capability significantly simplifies the assay procedure and minimizes the loss of rare pathogens.

To demonstrate its clinical utility, we applied the  $\mu$ Hall system to the detection of Gram-positive bacteria. The early diagnosis of such bacteria has become increasingly important with the emergence of drug-resistant strains (e.g., methicillin-resistant *S. aureus*/MRSA, vancomycin-resistant Enterococci, penicillin-resistant *Streptococcus pneumoniae*).<sup>[20-22]</sup> The following panel of Gram-positive bacteria were tested: *S. aureus*, *Enterococcus faecalis* (*E. faecalis*) and *Micrococcus luteus* (*M. luteus*). As a control group, the following Gram-negative species were used: *Klebsiella pneumoniae* (*K. pneumoniae*), *Moraxella catarrhalis* (*M. catarrhalis*), *Pseudomonas aeruginosa* (*P. aeruginosa*). Samples were prepared by spiking cultured bacteria in liquid media (see Experimental section), which were then labeled with vanc-TCO and fluorescent MNP-Tz. Although the media contained ample proteins (2% fetal bovine serum and 1 mg/ml bovine serum albumin), we observed little

changes in labeling efficiency, which confirmed the robustness of this bioorthogonal approach. Figure 3d summarizes the profiling results. Both the  $\mu$ Hall sensor and flow cytometry were able to reliably distinguish Gram-positive from Gram-negative species. The  $\mu$ Hall sensor, however, required a far smaller sample volume (1  $\mu$ L) than the flow cytometer (~500  $\mu$ L). The  $\mu$ Hall assay time per sample was ~1 hour (40 minutes for MNP labeling, 30 minutes for  $\mu$ Hall detection).

In summary, we have developed a new bacterial detection platform, the  $\mu$ Hall system, for point-of-care diagnosis. By combining recent advances in magnetic nanomaterials and microelectronics, the  $\mu$ Hall system offers the following key advantages: 1) minimal sample processing and robust detection in different biological backgrounds (e.g., pH, salinity, turbidity); 2) high-throughput detection ( $10^7$  cells/minutes) and high resolution (single cell); and 3) simple and automatic diagnosis using a compact and self-contained device. As a proof-of-principle, we demonstrated the system's capability for universal detection of Gram-positive bacteria using vancomycin as the targeting ligand. By using different affinity ligands, the system could ultimately be adapted to specifically detect a variety of different pathogens (e.g., by using antibodies)<sup>[23]</sup> and to the more comprehensive detection of bacteria (e.g., by using a Gram-staining equivalent).<sup>[24]</sup> Moreover, the  $\mu$ Hall sensors can be implemented into a monolithic integrated circuit (IC) chip. By incorporating a large number of sensors and control circuits, the IC chip could provide superior throughput and obviate the need for microfluidics. Such a system would represent a powerful diagnostic tool with significant potential for controlling infectious diseases and promoting public health.

## Experimental section

### Fabrication of $\mu$ Hall device, magnetic simulation of $\mu$ Hall sensing, and preparation of labeling agents

This information is described in the SI Methods.

### Bacterial sources and culture

All bacteria were purchased from American Type Culture Collection (ATCC; Manassas, VA). The following media were used for suspension culture of each bacterial species: *Staphylococcus aureus* (#BAA-1721) in Staphylococcus broth (BD Biosciences), *Enterococcus faecalis* (#29212) in tryptic soy broth (BD Biosciences) containing 5% defibrinated sheep blood (Hemostat Laboratories), *Micrococcus luteus* (#147) in nutrient broth (BD Biosciences), *Pseudomonas aeruginosa* (#142) and *Klebsiella pneumoniae* (#BAA-2146) in tryptic soy broth, and *Moraxella catarrhalis* (#8176) in brain heart infusion broth (Sigma-Aldrich).

### Bacteria labeling

Bacteria in culture media were first washed with PBS containing 2% fetal bovine serum and 1 mg/ml bovine serum albumin (PBS++). For labeling, bacterial cells were added with vanc-TCO (20  $\mu$ M) and incubated at room temperature for 20 min. After washing 3 times with PBS++, MNP-Tz was added (50  $\mu$ g/ml) and incubated at room temperature for 20 minutes. Unreacted MNPs were removed by washing 3 times with PBS++, and fixed in 10%

paraformaldehyde for 20 minutes. Flow cytometry was performed using LSRII (BD Biosciences).

### Bacterial detection using the $\mu$ Hall system

The  $\mu$ Hall device was connected to a custom-designed electronic system that biases the  $\mu$ Hall sensors and acquires the Hall signal.<sup>[10]</sup> Each  $\mu$ Hall sensor was capacitively coupled to a preamplifier through a high-pass filter ( $f_{3dB} = 500$  Hz). A cascaded amplifier conditioned the signal (THS4131, Texas Instruments), with a gain of  $30 \times 30$ . The signal was then digitized ( $2.5 \times 10^6$  samples/s; PCI-6133, National Instruments) and analyzed by custom-developed software. A typical value for the bias current was 2 mA. The external magnetic field ( $\sim 0.5$  T) was produced by a neodymium magnet ( $\sim 1$  cm<sup>3</sup>) attached below the chip. The sample and sheath flow were delivered to the chip via three independent syringe pumps (BS8000, Braintree Scientific).

### Supplementary Material

Refer to Web version on PubMed Central for supplementary material.

### Acknowledgments

We thank N. Sergeev for the synthesis of cross-linked dextran iron oxide nanoparticles; C. Min, H. Shao and M. Liang for their helpful discussions; Y. Fisher-Jeffes for critically reviewing the manuscript; R.M. Westervelt (Harvard) for generously supporting fabrication of the device. This work was supported in part by NHLBI grants R01-HL113156 (H.L.), NIBIB R01-EB010011 (R.W.), R01-EB00462605A1 (R.W.), NHLBI contract HHSN268201000044C (R.W.), and T32CA79443 (R.W.).

### References

1. Batt CA. *Science*. 2007; 316:1579. [PubMed: 17569853]
2. Chin CD, Linder V, Sia SK. *Lab Chip*. 2007; 7:41. [PubMed: 17180204]
3. Enserink M. *Science*. 2001; 294:1266. [PubMed: 11701907]
4. Chin CD, Laksanasopin T, Cheung YK, Steinmiller D, Linder V, Parsa H, Wang J, Moore H, Rouse R, Umvilighozo G, Karita E, Mwambarangwe L, Braunstein SL, van de Wiggert J, Sahabo R, Justman JE, El-Sadr W, Sia SK. *Nat Med*. 2011; 17:1015. [PubMed: 21804541]
5. Luo PG, Stutzenberger FJ. *Adv Appl Microbiol*. 2008; 63:145. [PubMed: 18395127]
6. Phillips RL, Miranda OR, You CC, Rotello VM, Bunz UH. *Angew Chem Int Ed Engl*. 2008; 47:2590. [PubMed: 18228547]
7. Zhao X, Hilliard LR, Mechery SJ, Wang Y, Bagwe RP, Jin S, Tan W. *Proc Natl Acad Sci U S A*. 2004; 101:15027. [PubMed: 15477593]
8. Loureiro J, Andrade PZ, Cardoso S, da Silva CL, Cabral JM, Freitas PP. *Lab Chip*. 2011; 11:2255. [PubMed: 21562656]
9. Gaster R, Xu L, Han SJ, Wilson R, Hall D, Osterfeld S, Yu H, Wang S. *Nat Nanotechnol*. 2011; 6:314. [PubMed: 21478869]
10. Issadore D, Chung J, Shao H, Liang M, Ghazani AA, Castro CM, Weissleder R, Lee H. *Sci Transl Med*. 2012; 4:141ra92.
11. Liu P, Skucha K, Duan Y, Megens M, Kim J, Izyumin I, Gambini S, Boser B. *Solid-State Circuits. IEEE Journal of*. 2012:1.
12. Adams JD, Kim U, Soh HT. *Proc Natl Acad Sci USA*. 2008; 105:18165. [PubMed: 19015523]
13. Chung HJ, Reiner T, Budin G, Min C, Liang M, Issadore D, Lee H, Weissleder R. *ACS Nano*. 2011; 5:8834. [PubMed: 21967150]
14. Lee H, Yoon TJ, Weissleder R. *Angew Chem Int Ed Engl*. 2009; 48:5657. [PubMed: 19554581]

15. Devaraj NK, Upadhyay R, Haun JB, Hilderbrand SA, Weissleder R. *Angew Chem Int Ed Engl.* 2009; 48:7013. [PubMed: 19697389]
16. Schoch J, Ameta S, Jäschke A. *Chem Commun (Camb).* 2011; 47:12536. [PubMed: 22002170]
17. Haun JB, Devaraj NK, Hilderbrand SA, Lee H, Weissleder R. *Nat Nanotechnol.* 2010; 5:660. [PubMed: 20676091]
18. Haun JB, Castro CM, Wang R, Peterson VM, Marinelli BS, Lee H, Weissleder R. *Sci Transl Med.* 2011; 3:71ra16.
19. Yang R, Feedback DL, Wang W. *Sensors and Actuators A: Physical.* 2005; 118:259.
20. Arias CA, Mendes RE, Stilwell MG, Jones RN, Murray BE. *Clin Infect Dis.* 2012; 54(Suppl 3):S233. [PubMed: 22431854]
21. Menichetti F. *Clin Microbiol Infect.* 2005; 11(Suppl 3):22. [PubMed: 15811021]
22. Woodford N, Livermore DM. *J Infect.* 2009; 59(Suppl 1):S4. [PubMed: 19766888]
23. Liong M, Fernandez-Suarez M, Issadore D, Min C, Tassa C, Reiner T, Fortune SM, Toner M, Lee H, Weissleder R. *Bioconjug Chem.* 2011; 22:2390. [PubMed: 22043803]
24. Budin G, Chung HJ, Lee H, Weissleder R. *Angew Chem Int Ed Engl.* 2012; 51:7752. [PubMed: 22744868]

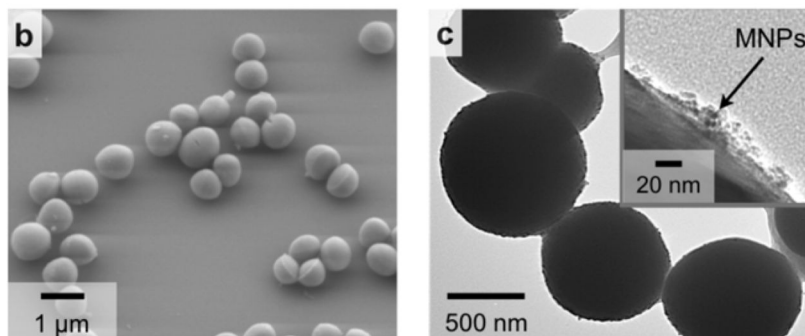
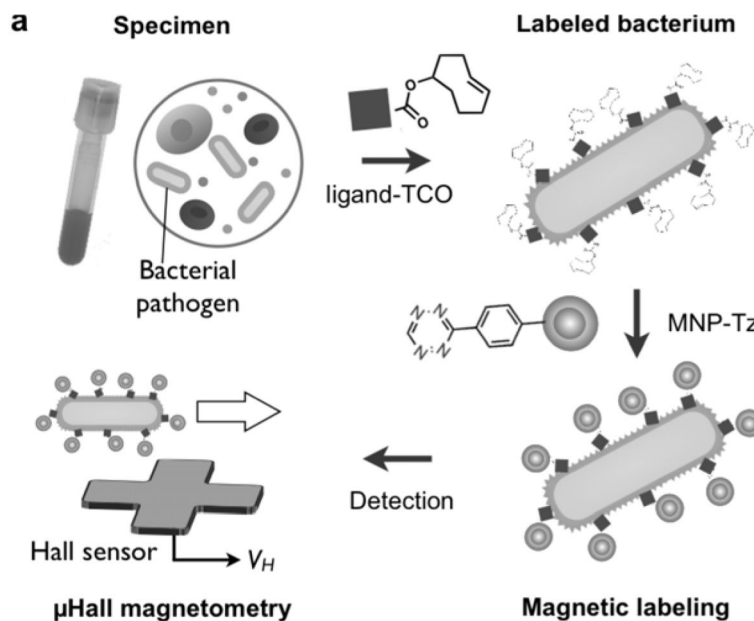


**Figure 1. Magnetic detection of individual pathogens with the  $\mu$ Hall sensor**

(a) Bacterial targets were labeled using affinity ligands modified with *trans*-cyclooctene (TCO). Magnetic nanoparticles (MNPs)-functionalized with tetrazine (Tz) were then introduced. MNP-labeled bacteria were detected using the micro-Hall ( $\mu$ Hall) sensor, which reports the voltage signal ( $V_H$ ) of each passing bacterium; this value is proportional to the number of MNPs bound to individual pathogens. (b, c) *Staphylococcus aureus* (*S. aureus*) was used as a detection target. The average diameter of *S. aureus* is  $\sim 1 \mu\text{m}$  (b). Bacteria were magnetically labeled using the antibiotic, vancomycin, as the affinity ligand. Transmission electron microscopy (c) confirmed MNP-binding to the bacterial membrane.



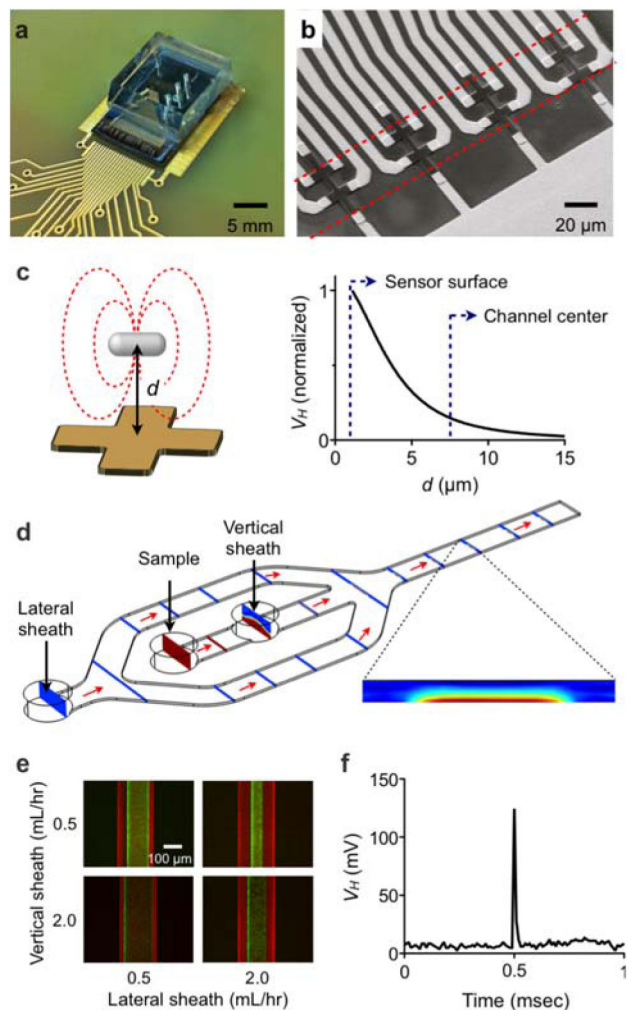


**Figure 2. Design and implementation of the bacterial  $\mu$ Hall sensor**

(a) A photograph of the  $\mu$ Hall device shows an array of  $\mu$ Hall sensors incorporated onto a semiconductor substrate with polydimethylsiloxane (PDMS) microfluidics directly on top. (b) Eight  $\mu$ Hall sensors, each measuring  $8\ \mu\text{m} \times 8\ \mu\text{m}$  were arranged into an overlapping array across the fluidic channel. The dotted lines indicate the width of the sample flow. (c) The signal  $V_H$  was simulated as a function of the vertical distance  $d$  between the center of a bacterium and the surface of the Hall sensor. Away from the sensor surface, the signal strength decayed rapidly ( $\sim d^{-3}$ ). (d) To enhance the  $\mu$ Hall signal, a hydrodynamic focusing structure was used to bring individual pathogens close to the  $\mu$ Hall sensor. With hydrodynamic focusing, bacteria entering the chip through the sample input port were pushed to the bottom of the channel by the vertical sheath flow (flow rate,  $S_V$ ) and focused towards the center of the channel by the lateral sheaths (flow rate  $S_L$ ). The finite-element simulation shows the focusing of bacteria to a region of  $\sim 100\ \mu\text{m} \times 7.5\ \mu\text{m}$ , within a physical channel measuring  $200\ \mu\text{m} \times 15\ \mu\text{m}$ . The flow rates were:  $S_V = 3S$  and  $S_L = 8S$ , where  $S$  is the sample flow rate. (e) A fluorescence micrograph of hydrodynamic focusing shows that focusing can be controlled by varying the relative flow rates between the vertical and lateral

sheaths. **(f)** With flow focusing, robust  $V_H$  signals from individual bacteria could be observed. The graph shows the  $V_H$  of a single *S. aureus* passing over a  $\mu$ Hall sensor.

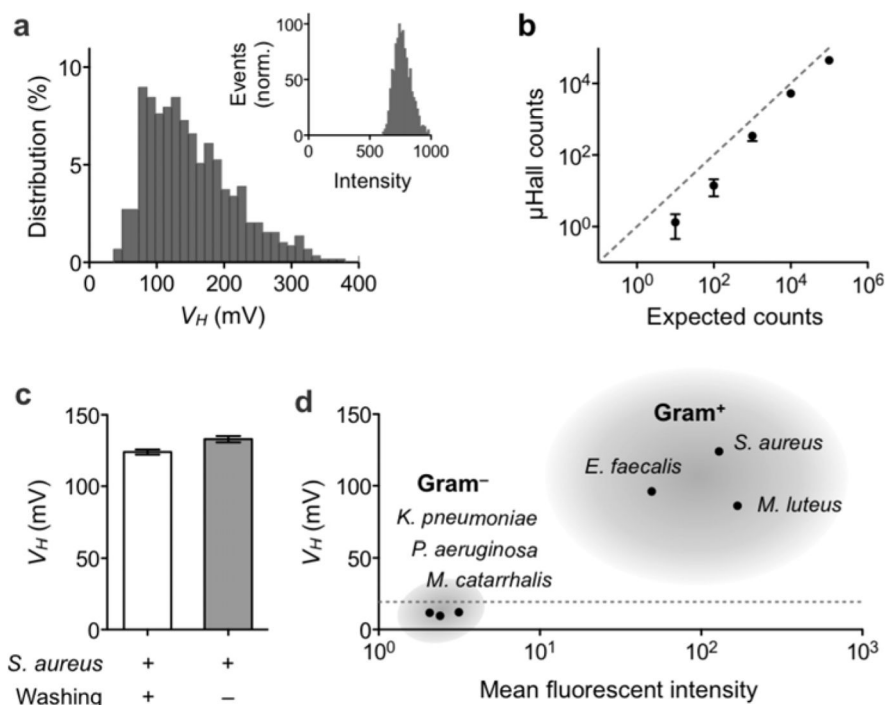


### Figure 3. System validation

(a) *S. aureus* was labeled using vancomycin (vanc)-TCO and fluorescent MNP-Tz. The Hall voltage distribution, as measured by the  $\mu$ Hall device, qualitatively matched with measurements by flow cytometry (inset). (b) The  $\mu$ Hall was used to count bacteria over wide dynamic ranges. Data are displayed as means  $\pm$  SEM of triplicate measurements. (c) *S. aureus* could be detected in the presence of excess unbound MNPs. Indeed, the measured signals were comparable to those from MNP-washed samples. (d) The  $\mu$ Hall sensor was used to detect Gram-positive bacteria. A panel of bacterial samples were labeled with vanc-TCO and fluorescent MNP-Tz. All Gram-positive bacteria (*S. aureus*, *E. faecalis*, *M. luteus*) showed high  $V_H$  values, whereas the  $V_H$  for Gram-negative species (*P. aeruginosa*, *M. catarrhalis*, *K. pneumoniae*) was  $< 20$  mV (dotted line). These  $\mu$ Hall results showed good agreement with flow cytometry data. The  $\mu$ Hall data is displayed as mean  $\pm$  SEM of 5000  $V_H$  values.